Dalton Transactions

RSC Publishing

Influencing the coordination mode of tbta (tbta = tris[(1-benzyl-1*H*-1,2,3-triazol-4-yl)methyl]amine) in dicobalt complexes through changes in metal oxidation states†

David Schweinfurth,[a] Johannes Klein,[b] Stephan Hohloch,[a] Sebastian Dechert,[c] Serhiy Demeshko,[c] Franc Meyer[c] and Biprajit Sarkar*[a]

The complexes [(tbta)Co(μ-CA$_{-2H}$)Co(tbta)(CH$_3$CN)](BF$_4$)$_2$ **1** and [(tbta)Co(μ-OH)$_2$Co(tbta)](BF$_4$)$_4$ **2** (tbta = tris[(1-benzyl-1*H*-1,2,3-triazol-4-yl)methyl]amine and CA = chloranilic acid) were synthesized and characterized by X-ray crystallography, SQUID magnetometry and NMR spectroscopy. The reactions to form these complexes deliver **1** as a paramagnetic species containing two high spin Co(II) centers, and **2** as a diamagnetic compound with two low spin Co(III) centers. Structural analysis shows that in **1** the capped-octahedral environment around the Co(II) centers is highly distorted with rather long bonds between the metal and donor atoms. The tbta ligand binds to the Co(II) centers through the three triazole nitrogen donor atoms in a facial form, with the Co–N(amine) distance of 2.494(2) Å acting as a capping bond to the octahedron. In the crystal an unusual observation of one acetonitrile molecule statistically occupying the coordination sites at both Co(II) centers is made. **1** displays a series of intermolecular C–H···Cl and π–π interactions leading to extended three-dimensional structures in the solid state. These interactions lead to the formation of voids and explain why only one acetonitrile molecule can be bound to the dinuclear complexes. In contrast to **1**, the cobalt centers in **2** display a more regular octahedral environment with shorter cobalt–donor atom distances, as would be expected for a low spin Co(III) situation. The tbta ligand acts as a perfect tetradentate ligand in this case with the cobalt–N(amine) distance of 2.012(3) Å falling in the range of a normal bond. Thus, we present the rare instances where the ligand tbta has been observed to bind in a perfectly tetradentate fashion in its metal complexes. The room temperature magnetic moment of 6.30 μ_B for **1** shows values typical of two high spin Co(II) centers, and this value decreases at temperatures lower than 30 K indicating a weak antiferromagnetic coupling and zero field splitting. Mass spectrometric analysis of **2** provided evidence for the formation of an oxo-bridged dicobalt complex in the gas phase.

Introduction

The ligand tris[(1-benzyl-1*H*-1,2,3-triazol-4-yl)methyl]amine, tbta (Scheme 1),[1] is a prominent example of the emerging class of tripodal ligands[2] that can be synthesized by the Cu(I) catalyzed "Click" reaction[3] between azides and alkynes. Interestingly, tbta was one of the first ligands that was used as an additive to enhance the efficiency of the "Click" catalytic processes,[1b,c] and subsequently structural elucidation of the involved Cu(I)-tbta complexes was made.[1d] Metal complexes of various substituted triazole ligands generated through the "Click" process are meanwhile well-known,[4] and have found applications in diverse fields of chemistry.[5,6] In the free form, 1,2,3-triazoles have been shown to have a particularly acidic C–H bond, thus allowing them to act as anion-binders by forming strong hydrogen bonds.[7] Molecular recognition through weak non-covalent interactions is a topic of immense current interest in contemporary chemistry.[8]

Chloranilic acid, CA (Scheme 1), in its various deprotonated forms is a frequently used bridging ligand with examples of mono- and dinuclear complexes, as well as coordination polymers being well-known in the literature.[9] Dicobalt complexes with CA$_{-2H}$ have been investigated with respect to their

[a]*Institut für Chemie und Biochemie, Anorganische Chemie, Freie Universität Berlin, Fabeckstraße 34-36, D-14195 Berlin, Germany. E-mail: biprajit.sarkar@fu-berlin.de*
[b]*Institut für Anorganische Chemie, Universität Stuttgart, Pfaffenwaldring 55, D-70550 Stuttgart, Germany*
[c]*Institut für Anorganische Chemie, Georg-August Universität Göttingen, Tammanstraße 4, D-37077 Göttingen, Germany*
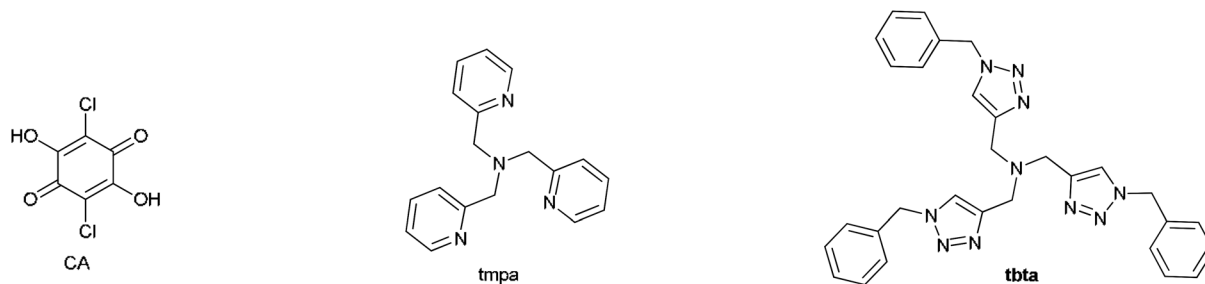
Scheme 1 CA, tmpa, and tbta.

magnetic properties, in particular in combination with the co-ligand tris(2-pyridylmethyl)amine, tmpa (Scheme 1).[10]

In these complexes as also in others,[9k] the tmpa ligand usually acts as a normal tetradentate ligand, binding to the metal center through all of its four nitrogen donor atoms. The ligand tbta is of course related to tmpa. Despite this similarity, to the best of our knowledge the only example of a metal complex where tbta acts as a real tetradentate donor towards one metal center has been reported for a 5-coordinated Cu(II) complex.[1d] Our own investigation of tbta with Fe(II) or Co(II) has shown it coordinating either through the three triazole donors, with the central amine forming only a weak bond, or through two triazole donors, and the central amine with one of the triazole arms remaining uncoordinated.[11] In the aforementioned Cu(I) complex used as a catalyst for the "Click" reaction, tbta was actually shown to act as a bridge between two metal centers in a dinuclear complex with one of the triazole rings binding to the metal centers through both its N donor atoms.[1d] The Fe(II) complex mentioned above is a high spin (HS) case, whereas the Co(II) complexes were reported in both HS and low spin (LS) states. In all these three states, the operation of the Jahn–Teller effect automatically enforces distortion of the octahedron around the metal centers.[12] However, despite these effects, tmpa is capable of acting as a regular tetradentate ligand for both HS Fe(II) and HS and LS Co(II).[10] Hence we were in the look-out for a similar coordination mode for the ligand tbta and to understand the circumstances under which tbta might actually act as a regular tetradentate ligand.

In the following, we present two very similar dicobalt complexes: a CA bridged dicobalt complex [(tbta)Co(μ-CA$_{-2H}$)Co-(tbta)(CH$_3$CN)](BF$_4$)$_2$, **1**, and a doubly hydroxide bridged dicobalt complex [(tbta)Co(μ-OH)$_2$Co(tbta)](BF$_4$)$_4$, **2**. Thus, both these complexes have tbta as co-ligands and oxygen-donating bridges that have an identical total charge. We explore the effect of changing the bridging ligand, with the same total charge in each case, on the oxidation and spin states of the cobalt centers. In turn, we investigate the effect of the oxidation and spin state of the cobalt centers on the coordination mode of the tbta ligand. We also point out the possibilities of weak interactions that arise on combining ligands such as CA and tbta, which provide enough sites for generating weak non-covalent intra- and intermolecular interactions, and explore the effects of such interactions on the

coordination number and mode of the cobalt centers. The bonding parameters of **1** will be compared to the corresponding complex [(tmpa)Co^{II}(μ-CA$_{-2H}$)Co^{II}(tmpa)](BF$_4$)$_2$ **3**[10b] that contains tmpa as a co-ligand. Results obtained from synthesis, single crystal X-ray diffraction, ^{1}H-NMR spectroscopy and SQUID magnetometry are discussed below to address the question formulated above.

Results and discussion

Synthesis and characterization

Complex **1** was synthesized by the addition of the deprotonated form of CA to a solution containing a mixture of Co-(BF$_4$)$_2$·6H$_2$O and tbta (Experimental section). **1** turned out to be paramagnetic, and was hence characterized by elemental analysis and single crystal X-ray diffraction. Despite the paramagnetic nature of **1**, we were not able to obtain interpretable EPR spectra of this molecule at the X-band. Attempts at using high-frequency and -field EPR, a technique known to deliver reliable spectra in cases where the X-band fails,[13] also did not help. This is probably related to the octahedral coordination of the Co(II) centers in **1** with their zero field splitting, coupled with the weak magnetic coupling between the two Co(II) centers in this dinuclear complex (*vide infra*). Investigation of the redox chemistry of **1** with cyclic voltammetry, in the hope of accessing a dicobalt(III) species, showed ill-defined, irreversible processes pointing to the decomposition of **1** on oxidation. A probable explanation for this phenomenon is the release of the CA$_{-2H}$ or the CH$_3$CN ligand on making the system electron poorer. The flexible binding of tbta is also likely to contribute to irreversible redox chemistry in these compounds. Oxidation of an HS Co(II) centre to Co(III) would intrinsically demand structural reorganization, however, this process can be reversible when appropriate co-ligands are used.[10b]

The failure to access a dicobalt(III) species in the case of **1** made us think about alternative strategies for generating a related dicobalt(III) species by keeping the total charge and kind of donor atoms of the bridging ligand constant. After investigating various routes, gratifyingly, the use of H$_2$O$_2$ together with a mixture of Co(BF$_4$)$_2$·6H$_2$O and tbta delivered the desired product in good yields. The compound **2**, formed in this process, is diamagnetic and was investigated by
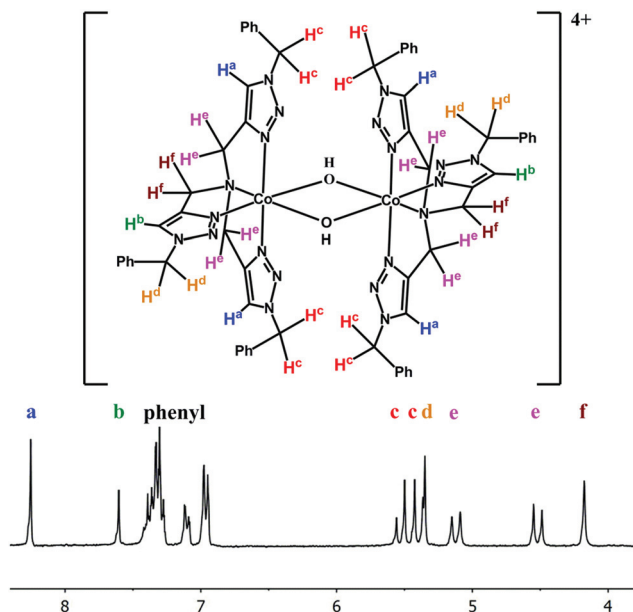
Fig. 1 ^{1}H-NMR spectrum of **2** in CD$_3$CN at 295 K.

^{1}H-NMR spectroscopy, single crystal X-ray diffraction, elemental analysis and mass spectrometry (Experimental section).

A detailed analysis of the ^{1}H-NMR spectrum of **2** provides useful insights into its structure in solution (Fig. 1). The number of signals and their splitting patterns can be explained by considering a local center of inversion as well as a local C_2 axis in the molecule in solution (overall C_{2h} symmetry). Thus, two different signals are observed for the ring C–H protons of the 1,2,3-triazole rings in a ratio of 2 : 1. The peak marked "a" is assigned to the triazole ring protons in the axial position, and the one marked "b" to the triazole ring protons in the equatorial position. These signals are low field shifted, as has been previously observed for other triazole C–H ring protons.[6a,b] The presence of three nitrogen atoms in the 1,2,3-triazole rings makes the C–H ring protons acidic, resulting in their down field shift.

The "CH$_2$" protons of the benzyl groups which are in the axial positions (marked c) deliver a splitting which is reminiscent of an AA'-pattern. This is a result of the geminal coupling between the protons of a "CH$_2$" group. A similar situation is observed for the "CH$_2$" protons attached to the amine nitrogen (marked e). An AA'-pattern resulting from a geminal coupling is observed for these axial protons as well. In contrast to the axial "CH$_2$" groups, the equatorial "CH$_2$" groups belonging to both the benzyl and the ones attached to the amines (marked d and f respectively) deliver singlets. The intensity ratios of these signals also help in their assignment. The benzyl "CH$_2$" (c and d) groups appear at lower fields compared to the "CH$_2$" groups attached to the central amine (e and f). The difference between the chemical shifts of the axial "CH$_2$" protons attached to the amine that undergo a geminal coupling is larger than the difference between the axial benzyl "CH$_2$" protons. This reflects a more drastic difference in the chemical

environments of the protons marked "e" compared to those marked "c". The phenyl protons of the benzyl groups appear as multiplets between 6.9 and 7.5 ppm. The "OH" protons of the bridge were observed in the ^{1}H-NMR spectrum of **2** at 0.63 ppm. Mass spectrometry and elemental analysis (Fig. 2 and Experimental section) confirmed the 4+ charge of the cation in **2**. Hence **2** contains two Co(III) centers bridged by two OH$^-$ ions and has neutral co-ligands. A direct proof of this came from X-ray crystallography (*vide infra*).

Interestingly, we were able to observe the 4+ charged cation of **2** in its ESI mass spectrum (Fig. 2). This is an unusual result considering the high charge of this cation. More intriguingly, a second peak was observed in the ESI mass spectrum which matched exactly with a 3+ cation that would be obtained from **2** after loss of a proton (Fig. 2). This result shows the possibility of deprotonating the hydroxo bridge of **2** in the gas phase to generate a dicobalt(III) complex that is bridged by one hydroxo and one oxo ligand.
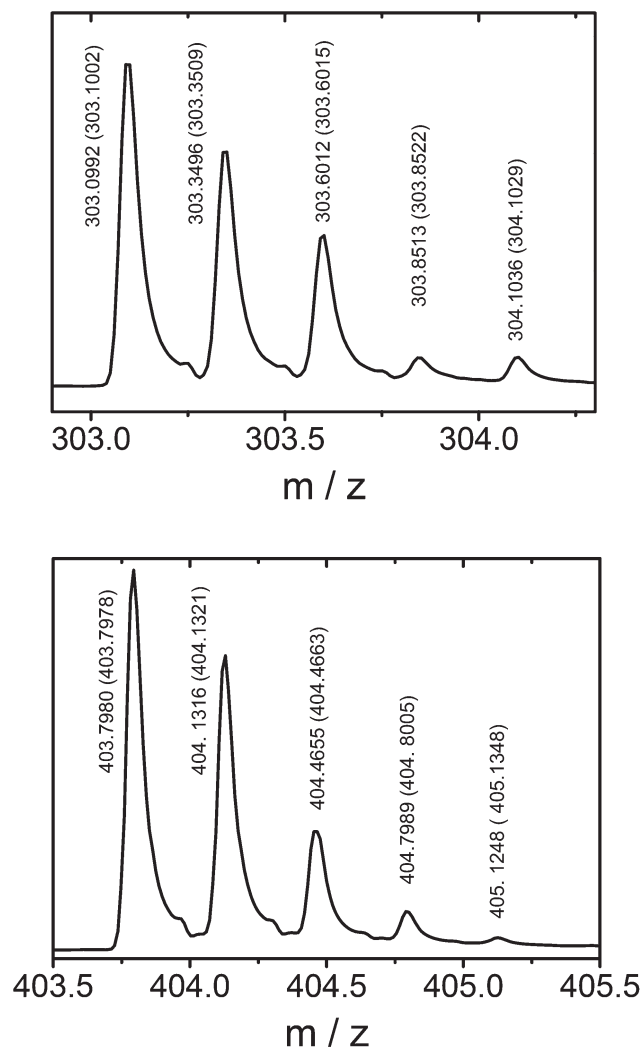

Fig. 2   ESI mass spectrum of [**2** − 4(BF$_4^-$)]$^{4+}$ (top) and [**2** − 4(BF$_4^-$) − H$^+$]$^{3+}$ (bottom). Simulated values are given in brackets.

The formation of **2** from its reaction components leads to some interesting observations. The reaction of a Co(II) salt in the presence of a tripodal-tetradentate ligand, tbta and H_2O_2 leads to the formation of the bis-hydroxo bridged dicobalt(III) compound **2** in good yields. The process of the formation of **2** thus likely involves the binding of H_2O_2 to two Co(II) centers, oxidation of each of the Co(II) centers to Co(III), transfer of the two electrons from the two cobalt centers to anti-bonding orbitals of H_2O_2, cleavage of the O–O bond in H_2O_2, and the formation of the bis-hydroxo bridged dicobalt(III) complex **2**. O–O bond cleavage together with oxidation of metal centers has precedence in oxygenation reactions that take place in biological systems.[14]

Crystal structures

Single crystals for both **1** and **2** could be obtained for X-ray diffraction studies. **1** crystallizes in the triclinic $P\bar{1}$ group (Table 1). The Co(II) centers in **1** are in a distorted capped octahedral environment, with each of the cobalt centres being coordinated by two oxygen donor atoms of the CA$_{-2H}$ bridge, and three of the triazole nitrogen donors of tbta (Fig. 3). For the sixth coordination position, only one acetonitrile ligand is found for both the Co(II) centres of each molecule. Such a situation leads to an unusual structure where only half of the Co(II) centres are coordinated to acetonitrile molecules. The capping bond is between the Co(II) centre and the central nitrogen atom of tbta.

The Co–N distances of about 2.1 Å (Table 2) to the triazole nitrogen donors are in the range observed for HS Co(II) complexes with tbta.[11] The Co–O distances are also in the expected range for an HS complex. The Co1–N1(amine) distance of 2.494(2) Å is on the longer side, but still consistent with a
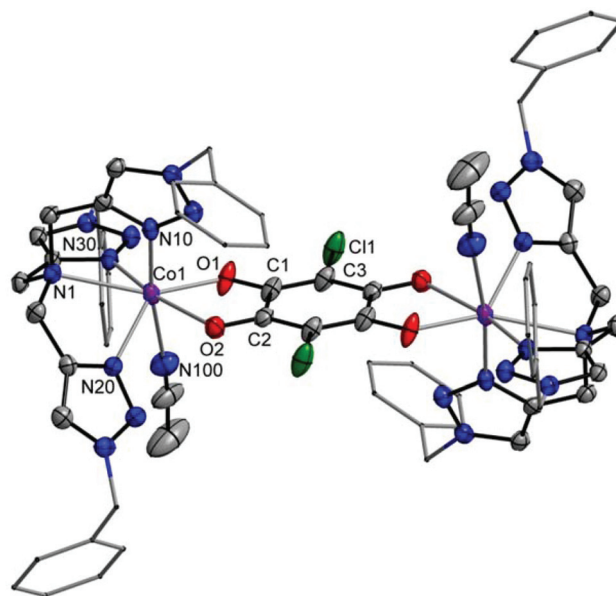

Fig. 3 ORTEP plot of **1**. Ellipsoids are drawn at 50% probability. Hydrogen atoms and counter-ions have been omitted for clarity. The CH_3CN molecules were calculated with a 50% probability at each site.

Table 2 Selected bond lengths (Å) for **1** and **2**

	1	**2**
Co1–O1	2.031(2)	1.905(2)/1.909(2)
Co1–O2	2.231(2)	—
Co1–N1	2.494(2)	2.012(3)
Co1–N10	2.100(2)	1.899(3)
Co1–N20	2.091(2)	1.908(3)
Co1–N30	2.122(2)	1.886(3)
Co1–N100	2.479(5)	
O1–C1	1.268(3)	
O2–C2	1.242(3)	
C1–C2	1.524(4)	
C1–C3	1.377(4)	
C2–C3	1.411(3)	

weak interaction of the amine nitrogen with the metal center. The tbta ligand is thus coordinated to the Co(II) centers through the three triazole N donors in a facial mode, with the amine nitrogen atom providing for a weak capping bond. Such a coordination mode for tbta has been observed for related HS Co(II) complexes earlier.[11] A look at the bond lengths within the CA$_{-2H}$ ligand shows that the C1–O1 bond at 1.268(3) Å is longer than the C2–O2 bond at 1.242(3) Å; accordingly, the C1–C3 bond at 1.377(4) Å is shorter than the C2–C3 bond at 1.411(3) Å. Such a bonding pattern shows the preference of the CA$_{-2H}$ ligand to act in a substituted *para*-quinone form in its metal complexes, with the negative charge showing a tendency to be localized at two oxygen atoms leading to a bis(alkoxy)-*p*-quinone type of ligand.

The angles between the donor atoms and the Co(II) centres in **1** (Table 3) show large deviations from the expected 90° and 180° angles. The chelating nature of the tbta and CA$_{-2H}$ ligands

Table 1 Crystallographic details for **1** and **2**

	1	**2**
Formula	$C_{72}H_{69}B_2Cl_2Co_2F_8N_{23}O_4$	$C_{60}H_{62}B_4Co_2F_{16}N_{20}O_2$
M_r	1682.88	1560.40
Crystal system	Triclinic	Orthorhombic
Space group	$P\bar{1}$	$Pbca$
a (Å)	11.2933(4)	21.184(2)
b (Å)	11.5315(4)	14.372(2)
c (Å)	16.4162(6)	22.001(3)
α (°)	108.969(3)	90
β (°)	91.903(3)	90
γ (°)	110.416(3)	90
V (Å^3)	1868.6(1)	6698(1)
Z	1	4
D_{calc} (g cm^{-3})	1.495	1.547
T (K)	133(2)	100(2)
μ (mm^{-1})	0.602	0.601
$F(000)$	864	3184
Meas./indep. refl.	25 772/7927	110 712/8309
Obsvd [$I > 2\sigma(I)$] refl.	6196	6352
R(int)	0.0511	0.0348
R [$F^2 > 2\sigma(F^2)$]	0.0482	0.0595
wR (F^2)	0.1058	0.1846
S	1.020	1.097
$\Delta\rho_{max}$, $\Delta\rho_{min}$ (e Å^{-3})	0.873, −0.696	2.400, −0.808

Table 3 Selected bond angles (°) for **1** (top) and **2** (bottom)

	1
O1–Co1–N20	133.05(9)
O1–Co1–N10	99.51(8)
N20–Co1–N10	112.85(8)
O1–Co1–N30	89.96(8)
N20–Co1–N30	112.71(8)
N10–Co1–N30	103.91(8)
O1–Co1–O2	75.01(7)
N20–Co1–O2	77.40(7)
N10–Co1–O2	81.09(8)
N30–Co1–O2	164.83(7)
O1–Co1–N100	72.3(1)
N20–Co1–N100	74.4(1)
N10–Co1–N100	171.8(1)
N30–Co1–N100	75.7(1)
O2–Co1–N100	97.3(1)
N1–Co1–N100	115.7(2)
N1–Co1–N10	71.34(8)
N1–Co1–N20	70.34(8)
N1–Co1–N30	71.18(8)
N1–Co1–O1	155.56(7)
N1–Co1–O2	123.83(7)
	2
N1–Co1–O1	178.3(1)
N10–Co1–N20	165.2(1)
N30–Co1–O1	176.4(1)
O1–Co1–O1	82.0(1)
O1–Co1–N10	97.1(1)
O1–Co1–N20	97.7(1)
O1–Co1–N30	96.5(1)
N1–Co1–O1	96.3(1)
N1–Co1–N10	82.3(1)
N1–Co1–N20	82.9(1)
N1–Co1–N30	85.2(1)
N30–Co1–N20	90.1(1)
N30–Co1–N10	88.1(1)
O1–Co1–N10	88.8(1)
O1–Co1–N20	93.4(1)

would intrinsically impose a certain amount of distortion to the metal centres. However, the extreme distortion from a perfect octahedron in the present case is also related to the capped octahedral geometry formed because of the weak Co–N(amine) bond, as well as the HS state of the Co(II) centers. The t_{2g} levels of an HS Co(II) center would experience Jahn–Teller distortion leading to a distortion of the (capped) octahedron around the Co(II) centre.[12]

Compound **1** has various positions predestined to undergo weak non-covalent interactions in the solid state. The C–Cl groups of the CA$_{-2H}$ ligand are known to form strong hydrogen bonds.[9o,p] The benzyl substituents of the tbta ligand,[11] as well as the C–H groups of the 1,2,3-triazole rings,[7] are known to undergo strong intra- and inter-molecular C–H···π and π···π interactions. For **1**, the C–H groups of the benzyl substituents form hydrogen bonds with the C–Cl groups of the neighboring molecules to form a two-dimensional chain (Fig. 4). Relevant distances and angles are C–H···Cl–C, 2.918 Å; C–H–Cl, 113.0° and H–Cl–C, 175.6°. These two dimensional chains are connected through π···π stacking between the phenyl rings of the benzyl groups (4.005 Å, Fig. 4) and the BF$_4^-$ counter-ions interacting with the C–H group of the 1,2,3-triazole rings (not shown in the figure).

The above-mentioned interactions lead to a situation where two of the dicobalt(II) complexes approach each other in the solid state in a way that leaves space for only one acetonitrile molecule per two Co(II) centers (Fig. 4). Such a situation might explain the unusual coordination geometry around the Co(II) centers discussed above. The Co–Co distance in **1** is 8.071(1) Å.

An interesting comparison can be made between compound **1** and the related complex **3**,[10] with tmpa as a co-ligand. Just like in **1**, the Co(II) centres in **3** are in the HS state. In keeping with this fact, the Co–O distances in **3** of 2.030(2) Å and 2.277(3) Å[10] are in the same range as that observed for **1** (Table 2). The average Co–N(pyridine) bond lengths in **3** are 2.1 Å,[10] a value that is in the same range as those for the average Co–N(triazole) bond lengths in **1** (Table 2). However, the Co–N(amine) distance of 2.494(2) Å in **1** is longer than the corresponding distance of 2.239(3) Å[10] observed in **3**. This longer Co–N(amine) bond to the tbta ligand in **1** makes the capped octahedron in **1** more distorted than the octahedron in **3**, and prevents a regular tetradentate bonding mode for tbta. The same weak Co–N(amine) bond in **1** is probably responsible for the coordination of an additional donating solvent molecule (CH$_3$CN), and the concomitant formation of a capped-octahedron type of coordination, a phenomenon not observed for **3**.

In contrast to **1**, the metal–ligand distances for **2** are all shorter (Fig. 5 and Table 2). The Co–O distances are 1.905(2) and 1.909(2) Å. The average Co–N(triazole) distance is 1.9 Å, a value that is 0.2 Å shorter than the corresponding distances in **1** (Table 2). Surprisingly, the Co–N1(amine) distance in **2** is 2.012 Å, a value that is 0.48 Å shorter than that in **1** (Table 2). The cobalt ions in **2** are in the LS +III oxidation state, and have a t_{2g}^6 configuration with no electrons in anti-bonding orbitals.[12] This leads to the shorter metal–ligand bonds, and helps the amine nitrogen to form a strong bond to the Co(III) centres. Additionally, octahedral LS Co(III) complexes do not show a Jahn–Teller distortion.[12] A combined result of these effects is the formation of shorter metal–ligand bonds, and angles between the cobalt centres and donor atoms that are closer to the 90° and 180° angles expected for a perfect octahedral case (Table 3). The possibility to form a regular octahedral geometry around the LS Co(III) centres contributes to the fact that tbta can act as a perfect tetradentate ligand in **2**, a coordination mode that has previously only been observed for a 1 : 1 mononuclear Cu(II) complex of tbta with an additional halide ligand.[1d] The distance between the two cobalt centers in **2** is 2.878(1) Å, a value that is comparable to other hydroxo-bridged dicobalt(III) complexes in the literature.[15] As has been mentioned above in the characterization part, all data for **2** point to the existence of LS Co(III) centres in **2**, and the structural data corroborate those facts.

Magnetic properties of 1

The magnetic properties of **1** were investigated by SQUID susceptometry. **1** has a room temperature magnetic moment of 6.30 μ_B which is in the range expected for two HS Co(II)
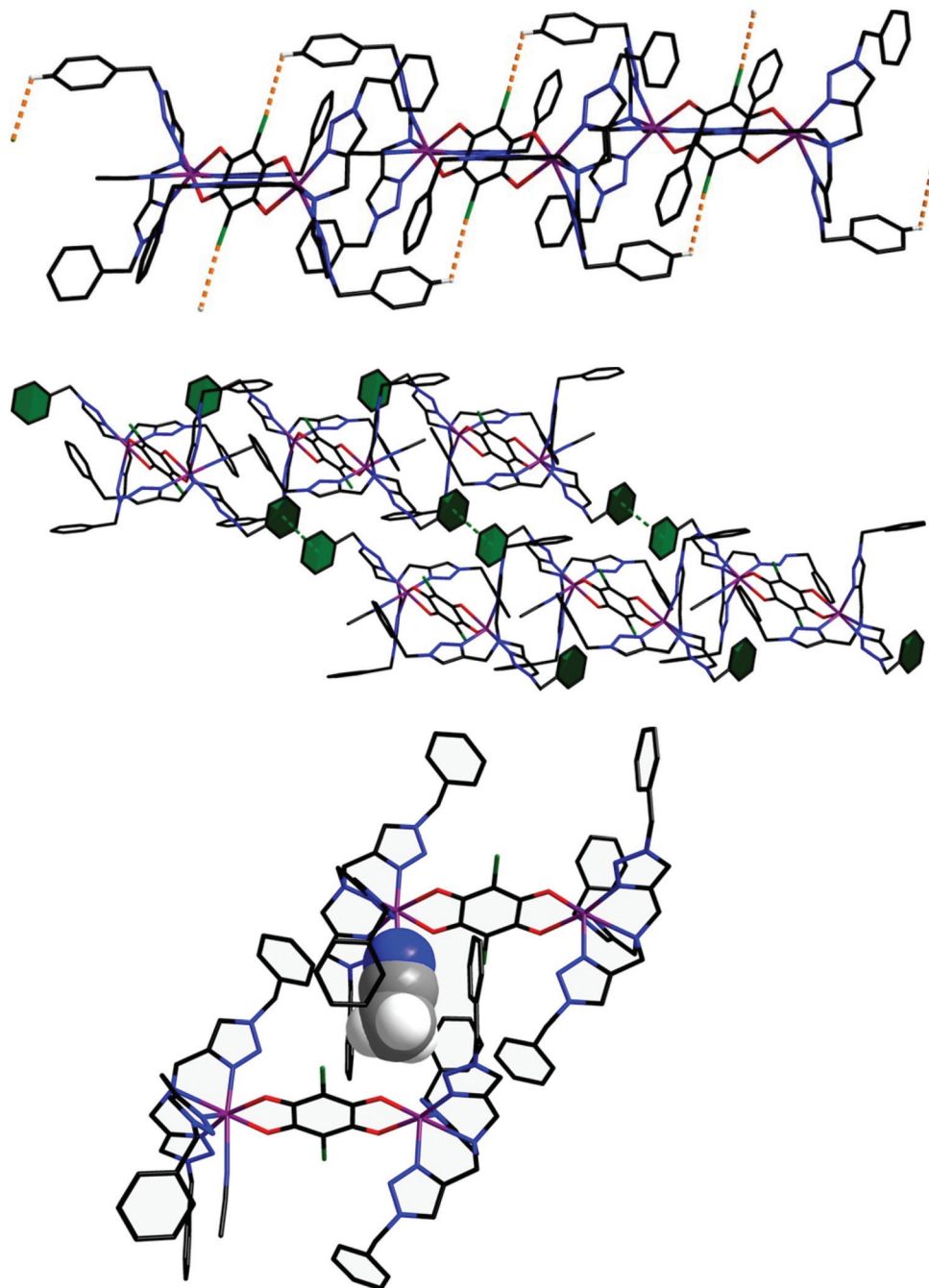
Fig. 4 Weak non-covalent inter-molecular interactions in **1** and the formation of voids to accommodate an acetonitrile molecule.

centers each with a spin of $S = 3/2$ and some orbital angular momentum contribution (5.48 μ_B for the spin-only case).[16] This value remains almost constant until 30 K, whereupon it decreases to 4.64 μ_B at 2 K (Fig. 6). The decrease of the magnetic moment value at lower temperatures is probably due to a combination of zero-field splitting observed for HS Co(II), and antiferromagnetic coupling between the two Co(II) ions. The temperature dependence of the magnetic data was modelled using a fitting procedure to the appropriate Heisenberg–Dirac–van Vleck spin Hamiltonian for two $S = 3/2$ cobalt centres with

isotropic exchange coupling, Zeemann splitting and zero-field splitting, eqn (1).

$$\hat{H} = -2J\hat{S}_1\hat{S}_2 + g\mu_B\vec{B}(\vec{S}_1 + \vec{S}_2) + \sum_{i=1}^{2} D_i\left(\hat{S}_{zi}^2 - \frac{1}{3}S_i(S_i + 1)\right) \quad (1)$$

The best fit parameters are $g = 2.27$, $J = -0.04$ cm^{-1} and $|D|$ = 9.8 cm^{-1}. The relatively small value of J reflects the weak (almost negligible) antiferromagnetic coupling in **1**, a result
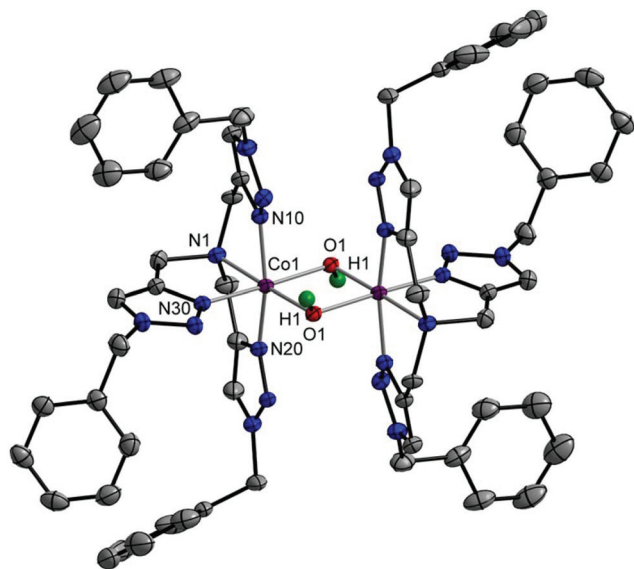
Fig. 5 ORTEP plot of **2**. Ellipsoids are drawn at 50% probability. Hydrogen atoms (except for OH) and counter-ions have been omitted for clarity.
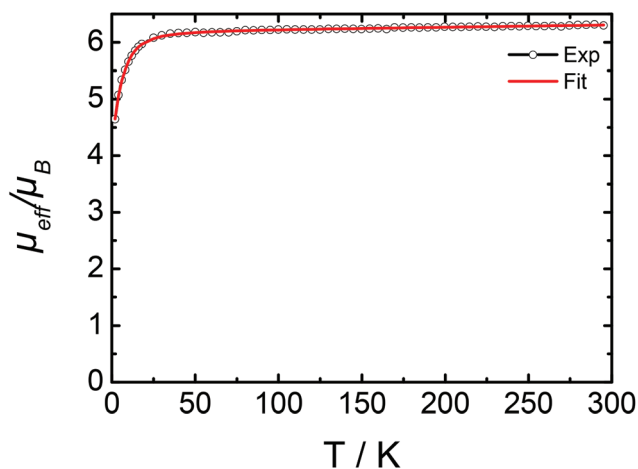

Fig. 6 Plot of the temperature dependence of the magnetic moment of **1** together with its fit.

which can be attributed to the large separation (more than 8 Å) between the two spin bearing Co(II) centres.[9o,p]

Conclusions

We have presented here two different cobalt complexes **1** and **2** that have the "Click" derived tbta as co-ligands. X-ray structural analyses of these compounds show that **1** contains two HS Co(II) centres where the metal centres adopt a capped octahedral type of coordination. The ligand tbta thus displays a 3 + 1 type of coordination in **1**. Additionally, in **1** only one acetonitrile ligand is found for two Co(II) centres, a result which has been explained by the formation of voids in the solid state through weak non-covalent intermolecular interactions between the CA-2H bridging ligand and the tbta co-ligands. Investigation of

the magnetic properties of **1** displayed characteristics of two weakly antiferromagnetically coupled HS Co(II) centres. **2** was synthesized by the oxidation of Co(II) with H_2O_2, with the subsequent cleavage of the O–O bond in H_2O_2 and the binding of OH^- as bridging ligands in **2**. In contrast to **1**, in **2** the cobalt centres are in the LS +III oxidation state. As a result of this, the metal-donor atom distances in **2** are all shorter than in **1**. A consequence of the octahedral LS +III state of the cobalt centres is the binding of tbta in **2** as a regular tripodal-tetradentate ligand. This is one of the rare occasions where such a coordination mode has been observed for tbta. Thus the delocalization of two negative charges over the CA-2H bridge in **1** leads to the formation of a bridge with weak ligand field strength, which leads to the stabilization of HS Co(II) centres. For **2** on the other hand, the concentration of negative charges on the two OH^- ligands leads to the stabilization of an LS Co(III) complex. It was also possible to generate oxo/hydroxo-bridged Co(III) species in the gas phase. The flexibility of the tbta ligand, as has been probed in the present case, would demand high reorganization energies during redox processes in complexes containing this ligand, and is probably responsible for the irreversible redox chemistry observed for **1**. Our present results display the versatile chemistry that can be generated with "Click" derived tripodal-triazole ligands, and also indicates possible applications of metal complexes containing such ligands in oxidation chemistry.

Experimental section

General

All solvents were dried and distilled using common techniques unless otherwise mentioned. The ligand tbta was synthesized by a reported procedure.[1a] ^{1}H-NMR spectra were recorded at 250.13 MHz on a Bruker AC250 instrument. Elemental Analyses were performed using a Perkin Elmer Analyser 240. Mass spectrometry measurements were carried out using an Agilent 6210 ESI-TOF instrument.

Syntheses

[(TBTA)Co-μ-CA-Co(TBTA)(CH₃CN)](BF₄)₂, 1. $Co(BF_4)_2 \cdot 6H_2O$ (100 mg, 0.29 mmol) and TBTA (156 mg, 0.29 mmol) were dissolved in CH_3CN (10 mL). The solution was stirred at room temperature for 1 h. Meanwhile, chloranilic acid (30 mg, 0.15 mmol) was dissolved in CH_3CN (10 mL) and deprotonated with NEt_3 (0.1 mL). The purple solution was added dropwise to the metal precursor solution and the resulting mixture was stirred for 5 min at room temperature. The product was crystallized by the addition of diethyl ether (20 mL). Dark red crystals suitable for X-ray diffraction were filtered, washed with ether and isolated in 40% yields (96 mg). Anal. Calcd for $C_{68}H_{63}B_2Cl_2Co_2F_8N_{21}O_4$: C, 51.02; H, 3.97; N, 18.38; Found C, 51.02; H, 4.17; N, 18.91. UV-Vis (ε (10^3 M^{-1} cm^{-1})): nm 333 (16.0), 377 (sh, 6.89), 538 (sh, 0.99). IR: cm^{-1} 1536, 1497, 1456, 1377, 1287, 1252, 1141, 1063, 1032, 1000, 966, 878, 849, 805, 762, 716, 650, 609, 577.

[(TBTA)Co-μ-(OH)₂-Co(TBTA)(CH₃CN)](BF₄)₄, 2. $Co(BF_4)_2 \cdot 6H_2O$ (64.2 mg, 0.19 mmol) and TBTA (100 mg, 0.19 mmol) were dissolved in acetonitrile (5 mL). The reaction mixture was stirred for 15 min and afterwards a 30% H_2O_2 solution (0.03 mL) was added. The solution was stirred overnight and the color changed from purple to red. Evaporation of the solvent gave a red oil, which was redissolved in minimum amounts of acetone. Because of the strong tendency of the compound to form an oil, ether was carefully added in the frequency of days to an acetone solution. The amount of ether was subsequently raised, in the frequency, till a red solid formed. It is difficult to report a correct yield of this compound because of its tendency to remain oily. Single crystals suitable for X-ray diffraction were grown by slow condensation of diethyl ether on top of an acetonitrile solution. Anal. Calcd for $C_{60}H_{62}B_4Co_2F_{16}N_{20}O_2$: C, 46.18; H, 4.01; N, 17.95; Found C, 45.38; H, 4.44; N, 18.00. MS (ESI): Calcd for $C_{60}H_{62}Co_2N_{20}O_2$ ($[M - (BF_4^-)_4]^{4+}$): m/z 303.1002; found 303.0992. Calcd for $C_{60}H_{61}Co_2N_{20}O_2$ ($[M - (BF_4^-)_4 - H^+]^{3+}$): m/z 403.7978; found 403.7980. ¹H-NMR (250 MHz, CD₃CN): δ 0.63 (s, 2H, OH), 4.18 (s, 4H, NCH_2), 4.52 (d, $^3J_{H-H}$ = 15.5 Hz, 4H, NCH(H)), 5.12 (d, $^3J_{H-H}$ = 15.1 Hz, 4H, NCH(H)), 5.35 (s, 4H, NCH_2), 5.39 (d, $^3J_{H-H}$ = 15.1 Hz, 4H, NCH(H)), 5.53 (d, $^3J_{H-H}$ = 15.0 Hz, 4H, NCH(H)), 6.97 (d, $^3J_{H-H}$ = 6.9 Hz, 8H, phenyl), 7.10 (d, $^3J_{H-H}$ = 7.7 Hz, 4H, phenyl), 7.25–7.45 (m, 18H, phenyl), 7.60 (s, 2H, triazole-CH), 8.25 (s, 4H, triazole-CH). ¹³C-NMR (176 MHz, CD₃CN): δ 150.72, 149.62, 134.55, 134.29, 130.20, 130.18, 130.17, 130.13, 128.89, 128.58, 127.93, 124.68, 61.96, 61.65, 57.16, 56.91. UV-Vis (ε (10^3 M^{-1} cm^{-1})): nm 303 (2.78), 501 (0.20). IR: cm^{-1} 3358, 3162, 2922, 2851, 1658, 1632, 1498, 1453, 1311, 1282, 1035, 932, 862, 807, 759, 728, 712, 659, 576.

Magnetic susceptibility measurements

Temperature-dependent magnetic susceptibility measurements were carried out with a *Quantum-Design* MPMS-XL-5 SQUID magnetometer equipped with a 5 Tesla magnet in the range from 295 to 2.0 K at a magnetic field of 0.5 T. The powdered sample was contained in a gel bucket and fixed in a non-magnetic sample holder. Each raw data file for the measured magnetic moment was corrected for the diamagnetic contribution of the sample holder and the gel bucket. Temperature-independent paramagnetism (TIP) and paramagnetic impurities ($S = 3/2$) were included according to $\chi_{calc} = (1 - PI) \times \chi + PI \times \chi_{mono} + TIP$; TIP = 610×10^{-6} cm^3 mol^{-1}, PI = 1% (fixed). Before simulation, the experimental data were corrected for TIP. The molar susceptibility data were corrected for the diamagnetic contribution. Magnetic properties were simulated using the *julX* program (E. Bill, Max Planck Institute for Chemical Energy Conversion, Mülheim/Ruhr, Germany).

X-ray crystallography

The intensity data were collected at 100(2) K on a Bruker Kappa Apex II duo diffractometer or at 133(2) K on a Stoe IPDS II. Crystallographic and experimental details of the structures are summarized in Table 1. The structures were solved by direct methods (SHELXS-97) and refined by full-matrix least-squares procedures (based on F^2, SHELXL-97).[17] The asymmetric unit of **1** contains a half molecule accompanied with a half occupied acetonitrile solvent molecule. CCDC 804874 and 911111 contain the cif files for this manuscript.

References

1 (a) J. E. Hein, L. B. Krasnova, M. Iwasaki and V. V. Fokin, *Org. Synth.*, 2011, **88**, 238; (b) T. R. Chan, R. Hilgraf, K. B. Sharpless and V. V. Fokin, *Org. Lett.*, 2004, **6**, 2853; (c) S. I. van Kasteren, H. B. Kramer, H. H. Jensen, S. J. Campbell, J. Kirkpatrick, N. J. Oldham, D. C. Anthony and B. G. Davis, *Nature*, 2007, **446**, 1105; (d) P. S. Donnelly, S. D. Zanatta, S. C. Zammit, J. W. White and S. J. Williams, *Chem. Commun.*, 2008, 2459.

2 (a) H. A. Michaels, C. S. Murphy, R. J. Clark, M. W. Davidson and L. Zhu, *Inorg. Chem.*, 2010, **49**, 4278; (b) C. Orain, N. Le Poul, A. Gomila, J.-M. Kerboal, N. Cosquer, O. Reinaud, F. Conan and Y. Le Mest, *Chem.–Eur. J.*, 2012, **18**, 594; (c) M. Jevric, T. Zheng, N. K. Meher, J. C. Fettinger and M. Mascal, *Angew. Chem., Int. Ed.*, 2011, **50**, 717; (d) S. Ozcubucku, E. Ozkal, C. Jimeno and M. Pericas, *Org. Lett.*, 2009, **11**, 4680.

3 (a) V. Rostovtsev, L. G. Green, V. V. Fokin and K. B. Sharpless, *Angew. Chem., Int. Ed.*, 2002, **41**, 2596; (b) C. V. Tornoe, C. Christensen and M. Meldal, *J. Org. Chem.*, 2002, **67**, 3057.

4 (a) L. Liang and D. Astruc, *Coord. Chem. Rev.*, 2011, **255**, 2933; (b) H. Struthers, T. L. Mindt and R. Schibli, *Dalton Trans.*, 2010, **39**, 675; (c) J. D. Crowley and D. McMorran in *Topics in Heterocyclic Chemistry*, ed. J. Kosmrlj, Springer, Berlin/Heidelberg, 2012, vol. 22, p. 31; (d) D. Schweinfurth, N. Deibel, F. Weisser and B. Sarkar, *Nachr. Chem.*, 2011, **59**, 937; (e) G. Aromi, L. A. Barrios, O. Roubeau and P. Gamez, *Coord. Chem. Rev.*, 2011, **255**, 485.

5 (a) Y. Li, J. C. Huffman and A. H. Flood, *Chem. Commun.*, 2007, 2692; (b) M. Ostermeier, M.-A. Berlin, R. M. Meudtner, S. Demeshko, F. Meyer, C. Limberg and S. Hecht, *Chem.–Eur. J.*, 2010, **16**, 10202; (c) W. W. Yang, L. Wang, Y. W. Zhong and Y. Yao, *Organometallics*, 2011, **30**, 2236; (d) K. N. Swanick, S. Ladouceur, E. Zysman-Colman and Z. Ding, *Chem. Commun.*, 2012, **48**, 3179; (e) D. G. Brown, N. Sanguantrakun, B. Schulz, U. S. Schubert and C. P. Berlinguette, *J. Am. Chem. Soc.*, 2012, **134**, 12354; (f) P. M. Guha, H. Phan, J. S. Kinyon, W. S. Brotherton, K. Sreenath, J. T. Simmons, Z. Wang, R. J. Clark, N. S. Dalal, M. Shatruk and L. Zhu, *Inorg. Chem.*, 2012, **51**, 3465; (g) J. D. Crowley and P. H. Bandeen,

Dalton Trans., 2010, **39**, 612; (*h*) D. Urankar, A. Pevec and J. Kosmrlj, *Cryst. Growth Des.*, 2010, **10**, 4920; (*i*) M. C. Clough, P. D. Zeits, N. Bhuvanesh and J. A. Gladysz, *Organometallics*, 2012, **31**, 5231; (*j*) K. A. Stevenson, C. F. C. Melan, O. Fleischel, R. Wang and A. Petitjean, *Cryst. Growth Des.*, 2012, **12**, 5169; (*k*) A. Maisonial, P. Serafin, M. Traikia, E. Debiton, V. Théry, D. J. Eitken, P. Lemoine, B. Viossat and A. Gautier, *Eur. J. Inorg. Chem.*, 2008, 298; (*l*) M. Mydlak, C. Bizzarri, D. Hartmann, W. Sarfert, G. Schmid and L. De Cola, *Adv. Funct. Mater.*, 2010, **20**, 1812; (*m*) S.-Q. Bai, S. Leelasubcharoen, X. Chen, L. L. Koh, J.-L. Juo and T. S. A. Hor, *Cryst. Growth Des.*, 2010, **10**, 1715; (*n*) R. Lalrempuia, N. D. McDaniel, H. Müller-Bunz, S. Bernhard and M. Albrecht, *Angew. Chem., Int. Ed.*, 2010, **49**, 9765; (*o*) K. J. Kilpin, U. S. D. Paul, A.-L. Lee and J. D. Crowley, *Chem. Commun.*, 2011, **47**, 328; (*p*) R. Saravanakumar, V. Ramkumar and S. Sankararaman, *Organometallics*, 2011, **30**, 1689.

6 (*a*) D. Schweinfurth, R. Pattacini, S. Strobel and B. Sarkar, *Dalton Trans.*, 2009, 9291; (*b*) D. Schweinfurth, S. Strobel and B. Sarkar, *Inorg. Chim. Acta*, 2011, **374**, 253; (*c*) S. Hohloch, C.-Y. Su and B. Sarkar, *Eur. J. Inorg. Chem.*, 2011, 3067; (*d*) D. Schweinfurth, C.-Y. Su, S.-C. Wei, P. Braunstein and B. Sarkar, *Dalton Trans.*, 2012, **41**, 12984.

7 Y. Hua and A. H. Flood, *Chem. Soc. Rev.*, 2010, **39**, 1262.

8 (*a*) S. Kubik, C. Reyheller and S. Stuwe, *J. Inclusion Phenom. Macrocyclic Chem.*, 2005, **52**, 137; (*b*) *Supramolecular Chemisty of Anions*, ed. A. Bianchini, K. Bowman-James and E. Garcia-Espana, Wiley-VCH, 1997; (*c*) J. L. Sessler, P. A. Gale and W.-S. Cho, *Anion Receptor Chemistry*, RSC Publishing, 2006.

9 (*a*) R. Ishikawa, Md. K. Kabir, K. Adachi, K. Nozaki and S. Kawata, *Chem. Lett.*, 2007, **36**, 1116; (*b*) K. Heinze, G. Huttner and O. Walter, *Eur. J. Inorg. Chem.*, 1999, 593; (*c*) S. Kawata, S. Kitagawa, M. Kondo, I. Furuchi and M. Munakata, *Angew. Chem., Int. Ed. Engl.*, 1994, **33**, 1759; (*d*) M. Kuwahara, Md. K. Kabir, K. Yamada, K. Adachi, H. Kumagai, Y. Narumi, K. Kindo, S. Kitagawa and S. Kawata, *Inorg. Chem.*, 2004, **43**, 92; (*e*) P. Gupta, A. Das, F. Basuli, A. Castineiras, W. S. Sheldrick, H. Meyer-Figge and S. Bhattacharya, *Inorg. Chem.*, 2005, **44**, 2081; (*f*) S. Gallert, T. Weyhermüller, K. Wieghardt and P. Chaudhuri, *Inorg. Chim. Acta*, 1998, **274**, 111;

(*g*) P. Chaudhuri and K. Oder, *J. Chem. Soc., Dalton Trans.*, 1990, 1597; (*h*) Y.-F. Han, W.-G. Gia, Y.-J. Lin and G.-X. Jin, *Organometallics*, 2008, **27**, 5002; (*i*) F. Tinti, M. Verdaguer, O. Kahn and J.-M. Savariault, *Inorg. Chem.*, 1987, **26**, 2380; (*j*) D. Guo and J. McCusker, *Inorg. Chem.*, 2007, **46**, 3257; (*k*) K. S. Min, A. L. Rheingold and J. S. Miller, *J. Am. Chem. Soc.*, 2006, **128**, 40; (*l*) A. Elduque, Y. Garcés, L. A. Oro, M. T. Pinillos, A. Tiripicchio and F. Ugozzoli, *J. Chem. Soc., Dalton Trans.*, 1996, 2155; (*m*) S. K. Jasimuddin, P. Byabartta, C. Sinha, G. Mostafa and T.-H. Lu, *Inorg. Chim. Acta*, 2004, **357**, 2015; (*n*) S. Ghumaan, B. Sarkar, S. Maji, V. G. Puranik, J. Fiedler, F. A. Urbanos, R. Jiminez-Aparicio, W. Kaim and G. K. Lahiri, *Chem.–Eur. J.*, 2008, **14**, 10816; (*o*) S. Kitagawa and S. Kawata, *Coord. Chem. Rev.*, 2002, **224**, 11; (*p*) Y.-F. Han, W.-G. Jia, W.-B. Yu and G.-X. Jin, *Chem. Soc. Rev.*, 2009, **38**, 3419; (*q*) Y.-F. Han, H. Li and G.-X. Jin, *Chem. Commun.*, 2010, **46**, 6879.

10 (*a*) K. S. Min, A. L. Rheingold, A. G. Dipasquale and J. S. Miller, *Inorg. Chem.*, 2006, **45**, 6135; (*b*) K. S. Min, A. G. Dipasquale, J. A. Golen, A. L. Rheingold and J. S. Miller, *J. Am. Chem. Soc.*, 2007, **129**, 2360.

11 (*a*) D. Schweinfurth, F. Weisser, D. Bubrin, L. Bogani and B. Sarkar, *Inorg. Chem.*, 2011, **50**, 6114; (*b*) D. Schweinfurth, S. Demeshko, M. M. Khusniyarov, S. Dechert, V. Gurram, M. R. Buchmeiser, F. Meyer and B. Sarkar, *Inorg. Chem.*, 2012, **51**, 7592.

12 J. R. Gispert, *Coordination Chemistry*, Wiley-VCH, Weinheim, Germany, 2008.

13 J. Telser, A. Ozarowski and J. Telser, *Electron Paramagnetic Resonance*, 2012, **23**, 209.

14 W. Kaim and B. Schwederski, *Bioinorganic Chemistry: Inorganic Elements in the Chemistry of Life*, Wiley-VCH, 1994.

15 (*a*) J. Luo, N. P. Rath and L. M. Mirica, *Inorg. Chem.*, 2011, **50**, 6152; (*b*) C. E. Sumner Jr., *Inorg. Chem.*, 1988, **27**, 1320; (*c*) K. Dimitrou, K. Folting, W. E. Streib and G. Christou, *J. Am. Chem. Soc.*, 1993, **115**, 6432; (*d*) D. A. Brown, W. Errington, W. K. Glass, W. Hasse, T. J. Kemp, H. Nimir, S. M. Ostrovsky and R. Wener, *Inorg. Chem.*, 2001, **40**, 5962; (*e*) R. Carballo, B. Covelo, E. M. Vázquez-Lopéz, E. Garcia-Martinez and A. Castineiras, *Z. Anorg. Allg. Chem.*, 2003, **629**, 584.

16 R. L. Carlin, *Transition Met. Chem.*, 1965, **1**, 1.

17 G. M. Sheldrick, *Acta Crystallogr., Sect. A: Found. Crystallogr.*, 2008, **64**, 112.